Vet. Res. (2010) 41:29
DOI: 10.1051/vetres/2010001

www.vetres.org

© INRA, EDP Sciences, 2010

Original article

Interferon-induced *Sus scrofa* Mx1 blocks endocytic traffic of incoming influenza A virus particles

Mélanie PALM, Mutien-Marie GARIGLIANY, François CORNET, Daniel DESMECHT*

Department of Pathology, University of Liège, FMV Sart Tilman B43, 4000 Liège, Belgium

(Received 9 October 2009; accepted 7 January 2010)

Abstract – The interferon-induced Mx proteins of vertebrates are dynamin-like GTPases, some isoforms of which can additionally inhibit the life cycle of certain RNA viruses. Here we show that the porcine Mx1 protein (poMx1) inhibits replication of influenza A virus and we attempt to identify the step at which the viral life cycle is blocked. In infected cells expressing poMx1, the level of transcripts encoding the viral nucleoprotein is significantly lower than normal, even when secondary transcription is prevented by exposure to cycloheximide. This reveals that a pretranscriptional block participates to the anti-influenza activity. Binding and internalization of incoming virus particles are normal in the presence of poMx1 but centripetal traffic to the late endosomes is interrupted. Surprisingly but decisively, poMx1 significantly alters binding of early endosome autoantigen 1 to early endosomes and/or early endosome size and spatial distribution. This is compatible with impairment of traffic of the endocytic vesicles to the late endosomes.

Mx / virus / interferon / endocytosis

1. INTRODUCTION

Nearly 50 years ago, the inbred mouse strain A2G was shown to be resistant to doses of mouse-adapted influenza A virus that were lethal to other inbred strains [15]. This innate resistance to experimental infection with influenza A viruses behaved as a single autosomal dominant trait [16]. Positional cloning of the relevant locus later revealed that the phenotype was encoded by a single gene on chromosome 16, coding for an approximately 75-kDa dynamin-like protein with GTPase activity: the Mx protein [29]. Close inspection of this gene revealed a correlation between the susceptibility of most inbred laboratory strains to orthomyxoviruses and either a premature stop codon or a large deletion spanning exon 9 to exon 11, both mutations leading to synthesis of a truncated Mx1 protein [37]. It soon became clear that the mouse Mx1 gene was only the first member of a small family of 1 to 3 genes present in all vertebrates. In all cases studied to date, expression of the Mx proteins is strictly subordinated to the presence of interferon IFNα/β. Only some isoforms exert antiviral activity, which further depends on their subcellular localization. Nuclear Mx proteins, observed only in rodents, inhibit orthomyxoviruses exclusively, whereas cytoplasmic Mx proteins display as a group a very broad antiviral spectrum suggestive of functional diversity. It is important to discover the mechanisms underlying these various antiviral activities. Such knowledge should open prospects of developing new antiviral drugs, which seems particularly important in the field of influenza A viruses. To our knowledge, four Mx isoforms capable of blocking the influenza A virus life cycle have been undisputedly identified to

* Corresponding author: daniel.desmecht@ulg.ac.be

This is an Open Access article distributed under the terms of the Creative Commons Attribution-Noncommercial License (http://creativecommons.org/licenses/by-nc/3.0/), which permits unrestricted use, distribution, and reproduction in any noncommercial medium, provided the original work is properly cited.

Article published by EDP Sciences

date: Mx1 of mouse [36], rat [2], swine [22] and the human MxA protein [26]. The only Mx whose anti-influenza action mechanism has been identified is the murine Mx1 protein, which blocks primary transcription of orthomyxoviruses via molecular interaction with the PB2 subunit of the viral polymerase [12, 40]. In our opinion, identifying the anti-influenza mechanisms of human MxA and porcine Mx1 (poMx1) should be a priority, because these proteins still inhibit the life cycle of influenza A virus after thousands of years of co-evolution. This suggests that the innate resistance mechanisms involved could be hard to fully bypass, even for a virus that is known for its genetic plasticity. These two Mx proteins localize to the cytoplasm, which prevents them from interfering with transcription, like murine Mx1. The only study to have addressed this question concluded that there must be a block downstream from primary transcription. More precisely, the production of viral transcripts, their polyadenylation, and their export from the nucleus to the cytoplasm were all intact in the presence of the human MxA protein [27]. Here the aim was to contribute to identifying the mechanism underlying the anti-influenza activity of poMx1. Our results are definitely compatible with the presence of a pre-transcriptional block, which confirms the functional diversity of the Mx proteins.

2. MATERIALS AND METHODS

2.1. Generation of the Vero cell clone producing poMx1 upon induction

The T-Rex technique (Invitrogen, Carlsbad, CA, USA) was used to generate double-transgenic Vero cell clonal lines showing tightly regulated conditional expression of poMx1 upon exposure to doxycycline. Vero cells (ATCC#CCL-81) grown at 37 °C in a 5% CO_2-air mixture in Dulbecco's modified Eagle's medium supplemented with 10% fetal bovine serum, 1% (v/v) penicillin-streptomycin and 0.5% amphotericin (DMEM/10) were first transfected with the expression plasmid pcDNA-TetR (Invitrogen) by the lipofectamine 2 000 procedure according to the manufacturer's instructions. Vero cells were chosen because their genetic defect in type I IFN production prevents activation of endogenous type I IFN-dependent effectors upon infection, thus allowing an artefact-free functional evaluation of exogenous Mx proteins [9]. Transfectants resistant to blasticidin (10 μg/mL) were recovered after 2 weeks of selection and cloned once by limiting dilution. Resulting clones were obtained after an additional 4-week round of blasticidin selection and screened for tightly controlled conditional expression by measurement of eGFP expression after transient transfection with our expression plasmid pcDNA4-eGFP [3] and detection by flow cytometry. A few clones combined intense fluorescence in the presence of 1 μg/mL doxycycline and total extinction without doxycycline. The transfectin technique was then used to transfect one of these clones (Vero/TetR1) with *Pvu*I-linearized pcDNA-poMx1α, our mammalian expression vector for the alpha isoform of poMx1 [24]. Transfected Vero/TetR1 cells were then seeded into DMEM/10 for 24 h without selection, after which blasticidin (10 μg/mL) and zeocin (350 μg/mL) were added. Blasticidin/zeocin-resistant double transfectants were recovered after 4 weeks of selection and cloned by limiting dilution.

The resulting clones were screened for poMx1 expression by combined immunofluorescence and immunoblotting. Immunofluorescence was carried out on induced (1 μg/mL) Vero/TetR1/poMx1 cell clones grown on coverslips. Cells were fixed with 4% (w/v) paraformaldehyde in phosphate-buffered saline (PBS) for 30 min at 4 °C, permeabilized in PBS/saponin (0.2% w/v), blocked for 1 h in PBS/saponin/BSA (1% w/v) at room temperature (RT), probed for 1 h at RT with a rabbit antiserum raised against human MxA (a kind gift from I. Julkunen, Finland), and after three washings, incubated for a further 1 h with relevant secondary antibodies conjugated to Alexa 488 (Molecular Probes, Merelbeke, Belgium). Processed coverslips were then screened with an Olympus BX51 epifluorescence microscope. For Western blot analysis, non-induced and induced (1 μg/mL doxycycline) Vero/TetR1/poMx1 cell monolayers were washed three times in PBS and harvested by trypsinization. Cell pellets were boiled for 5 min in loading buffer and aliquots were electrophoresed on a 4–12% SDS-polyacrylamide gel (Invitrogen). Proteins were then transferred onto a polyvinylidene difluoride membrane (Amersham Bioscience, Diegem, Belgium), and nonspecific binding blocked with 1% Western Blocking Reagent (Roche Bioscience, Vilvoorde, Belgium) at 4 °C overnight. Blocked membranes were probed with the anti-MxA rabbit antiserum diluted 1:1000 and with an anti-β-actin mAb in Tris-buffered saline

supplemented with 0.5% Western Blocking Reagent at 37 °C for 60 min. The membrane was then washed in TBS/Tween 20 (0.1% w/v) and incubated further with HRP-conjugated goat anti-rabbit and anti-mouse IgG (Cell Signaling Technology, Leiden, The Netherlands) at 37 °C for 60 min. Blots were then washed sequentially in PBS and distilled water and developed by incubation with 3-amino-9-ethylcarbazole (Dakocytomation, Heverlee, Belgium).

2.2. Viruses, infections, and virus-yield reduction assays

Two influenza A viruses, a porcine H1N1 virus (A/swine/Iowa/4/1976), and a H3N2 reassortant (X31) with the glycoproteins from A/Aichi/2/68 and the rest of the genes from the human mouse/egg-adapted A/PR/8/34 strain, were used in this study. The two viruses were propagated and stocks were produced and plaque-titered on Vero cells. For infections, stock aliquots were first diluted in DMEM supplemented with 0.2% BSA (Invitrogen) and 2 μg/mL trypsin-TPCK (Sigma-Aldrich, Bornem, Belgium). Serial dilutions were prepared just before use in order to generate volume-matched inoculums with appropriate multiplicities of infection. When the endocytic entry of influenza A viruses was targeted, a very high multiplicity of infection was used (> 150) to allow detection of incoming particles, as previously shown [8, 34]. Upon infection, viruses were allowed to adsorb for 60 min at 37 °C and then cell monolayers were thoroughly washed and incubated further with fresh DMEM/10. Infections were stopped, after predefined time intervals depending on the step of the viral cycle targeted, by incubation in 4% (w/v) paraformaldehyde in PBS for 30 min at 4 °C. Interference of poMx1 expression with the biological cycle of influenza A viruses was probed by flow cytometric detection of nucleoprotein (NP) synthesis in transiently transfected Vero cells and virus-yield reduction assays performed on induced and non-induced V50 cells. Transfection was performed according to the Transfectin technology (BioRad Laboratories, Nazareth, Belgium), essentially as described by the manufacturer, using a transfection mixture consisting of 50 μL MEM, 1 μL Transfectin and 50 μL MEM to which 0.75 μg of each plasmid DNA had been incorporated (pcDNA4-eGFP as negative control, pcDNA4-huMXA as positive control and pcDNA4-poMX1α as experimental group). Briefly, Vero cells were seeded in 24-well plates and grown overnight to 70–80% confluency. Then, cells were washed three times with PBS, medium was replaced with 200 μL MEM per well, and 100 μL of the transfection mixture was slowly incorporated in each well. Twenty-four hours after transfection, the cells were thouroughly washed three times with PBS and the infectious mixture was incorporated in each well, the target multiplicity of infection being ∼ 1. After a 60-min inoculum-cell contact for adsorption, the inoculum was removed by thorough washing with PBS and the cultures were incubated at 37 °C for 5 h in DMEM/2. Vero cells were then harvested by trypsinisation and pelleted at 300 *g* for 15 min. The cells were fixed with 4% (w/v) paraformaldehyde in PBS for 30 min at 4 °C, permeabilized in PBS to which 0.2% (w/v) saponin had been added and blocked for 1 h in PBS, 0.2% saponin and 1% (w/v) BSA at RT. Cells were then incubated for 45 min with a cocktail of primary antibodies, i.e. the polyclonal rabbit anti-huMxA antiserum and a monoclonal anti-NP antibody (Abcam, Belgium) at 37 °C. After three washing steps, the cells were incubated with the relevant Alexa 467- (NP) or 488-conjugated (Mx) secondary antibodies (Molecular Probes) at 37 °C. The immunolabelled cells were finally resuspended in PBS and analysed with the BD-Canto flow cytometer, gating on the forward and side scatter to exclude debris and collecting fluorescences in FL-1 and FL-5. A minimum of 10^4 events were acquired and analysed with the BDF-ACSDiva software v4.1.1.

For virus yield reduction assays in V50 cell monolayers, the infected cultures were incubated at 37 °C for 48 h in DMEM/2. The culture supernatants were sampled and viral titers determined in triplicate by standard median tissue culture infectious dose assays.

2.3. Quantification of transcripts encoding influenza A virus NP

Three hours after a standardized infection (H1N1, m.o.i. = 1), influenza A virus NP transcript levels were compared in monolayers of induced and non-induced V50 cells exposed or not to cycloheximide (100 μg/mL).

2.3.1. Production of cDNA samples

Infected V50 cell monolayers were individually homogenized (Qiagen's TissueLyser, 30 Hz for 5 min, Venlo, The Netherlands) in TRIzol (Invitrogen) for preparation of total mRNA. Each homogenate was treated with TURBO DNase (Ambion, Lennik, Belgium) for 30 min at 37 °C. After purification by use of the Invisorb Spin Cell RNA Minikit 50 according to the manufacturer's instructions (Invitek, Berlin, Germany), the purity and concentration

of each extract were determined spectrophotometrically (the OD260/280 and OD260/230, respectively, were in the ranges 1.9 → 2.0 and 1.8 → 2.2, NanoDrop-1000/Isogen) and mRNA integrity was checked by agarose gel electrophoresis. An aliquot of each condition-specific total RNA extract (2 µg RNA) was then reverse-transcribed at 42 °C for 60 min in the presence of 2 µL oligo-DTs (10 µM) and the ImProm II™ reverse transcription system (Promega, Leiden, The Netherlands).

2.3.2. Real-time PCR

The primer pairs used to amplify fragments of the viral NP transcripts and the probe used to detect the amplified fragments were as follows: 5′-ATCCTG GAATGCTGAAT-3′ (fwd), 5′-ACCAAACGAAA ATCCAGC-3′ (rev), and 5′-GCTCATAAGTCTTGC CTGCTTGTGTG-3′ (FAM-TAMRA). The PCR mixture consisted of template cDNA (1 µL), 100 nM primers (0.5 µL of each), 100 nM probe (0.5 µL), and 47.5 µL 1 × ABsolute™ QPCR ROX Mix (AB Gene, Leusden, The Netherlands) in a final volume of 50 µL. The mixture was placed in an ABI PRISM® 7700HT thermocycler and amplification was carried out under the following conditions: initial denaturation at 95 °C for 15 min, followed by 40 cycles of denaturation at 95 °C for 15 s and annealing-extension at 57 °C for 60 s, and then a final extension at 72 °C for 30 s. Amplification of transcripts was performed in triplicate, and three independent sessions were carried out with each RNA extract. The melting curve of each amplicon was monitored by means of a swing back to 50 °C, followed by a stepwise rise in temperature up to 95 °C. Melting curve analysis always revealed the presence of a single product. To check for false positives, RT-free and no-template controls were run for each template. Amounts of NP-encoding mRNA were normalized with respect to the amount of endogenous 18S ribosomal RNA, which was determined by use of the TaqMan® Ribosomal RNA Control Reagents kit (Applied Biosystems, Foster City, CA, USA).

2.4. Staining of virus proteins and host endosomes

2.4.1. Indirect immunofluorescence assays

Monoclonal antibodies raised against NP and pH-dependent specific conformations of HA were used to detect influenza A viruses, whereas a mAb targeting the early endosome autoantigen 1 (EEA1) protein was used to visualize early endosomes. Semiconfluent induced and non-induced V50 cells on coverslips were infected with the H1N1 or H3N2 influenza A virus. At predefined time points after infection, the cells were fixed with 4% (w/v) paraformaldehyde in PBS for 30 min at 4 °C, permeabilized as described above, and immunostained by sequential incubation with anti-NP mAb (Abcam), anti-HA mAb N2 or A2 (a kind gift from J.-M. With, University of California, USA) or anti-EEA1 mAb (Abcam), and then with AlexaFluor 488-conjugated goat anti-mouse IgG secondary antibodies (Molecular Probes). The immunolabeled cells were visualized with a laser scanning confocal microscope (Olympus).

2.4.2. Visualization of endocytosed membranes

For monitoring the fate of primary endocytic vesicles, V50 cell plasma membranes and virus envelopes were saturated with the lipophilic fluorescent dye DiD (1,1′-dioctadecyl-3,3,3′,3′-tetramethylindoldicarbocyanine, 4-chloro-benzenesulfonate salt, Molecular Probes) by incorporating the dye 20 min before adsorption of the virus. In this case, the cells were visualized directly after fixation.

3. RESULTS

3.1. Conditional expression of poMx1 in Vero cells

We sought to obtain Vero cells that would express poMx1 conditionally, in response to the presence of doxycycline in the medium. A series of 264 blasticidin/zeocin-resistant double-transgenic clones was screened. Immunofluorescence staining was used to determine, for each clone, (i) the proportion of cells expressing poMx1 when grown in doxycycline-free medium, (ii) the proportion of cells expressing poMx1 upon induction, and (iii) the subcellular intensity of poMx1 staining. Only one clone (hereafter referred to as V50) combined less than 5% spontaneous expression with more than 95% expression and intense cytoplasmic granular staining upon exposure to doxycycline. The clone was characterized further by Western blotting, which confirmed synthesis of an approximately 74-kDa protein recognized by human-MxA-specific antiserum (Fig. 1). The pattern of poMx1 expression

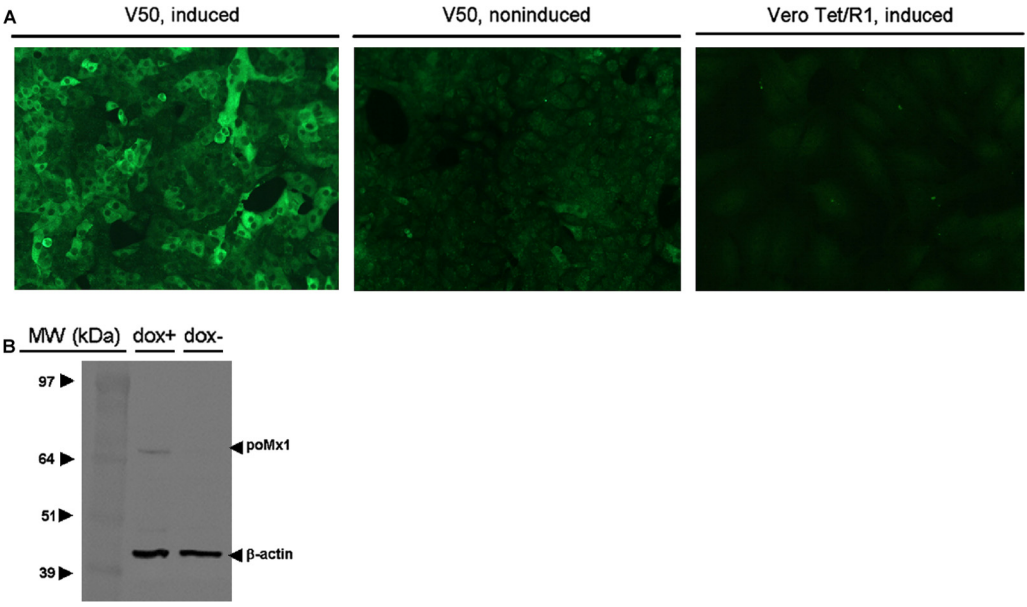

Figure 1. Expression of poMx1 in double-transgenic Vero cells examined by fluorescence microscopy and immunoblotting (clone V50). Transgenic cells were induced with 1 μg/mL doxycycline for 24 h. Induced mono-transgenic cells (clone Vero Tet/R1) are presented for control purposes (low background and absence of cross-reactivity with endogenous *Cercopithecus aethiops* Mx). Clone V50 combined less than 5% spontaneous expression with more than 95% expression and intense cytoplasmic granular staining upon exposure to doxycycline. The Western blot reveals a specific band in the lane for induced cells. The molecular mass corresponding to this band is compatible with that of poMx1 (74 kDa). For indirect immunofluorescence (A), cells were permeabilized and stained by sequential incubation with a rabbit antiserum raised against human MxA (a gift from I. Julkunen, Helsinki, Finland), which had been shown to cross-react with porcine Mx1 [24], and with Alexa 488-conjugated goat anti-rabbit IgG. (B) Immunoblots of 4–12% sodium dodecyl sulfate polyacrylamide gels with total cell proteins extracted from induced (dox +) and non-induced (−) V50 cells (10 μg total protein per lane, as determined by a micro-BCA assay). Immunostaining was done by sequential incubation with a cocktail of the above-mentioned rabbit antiserum and anti-β-actin mAb and a mix of HRP-conjugated anti-rabbit and anti-mouse IgG. Blots were developed by incubation with 3-amino-9-ethylcarbazole. The positions of protein size markers in kilodaltons are indicated (MW). (A color version of this figure is available on line at www.vetres.org.)

remained stable over 30 days of culturing with passaging every 3–5 days as needed. Sequencing of the product amplified from induced V50 extracts by poMx1-specific RT-PCR yielded the authentic poMx1 CDS.

3.2. Influenza A virus NP synthesis and infectious particle production are blocked upon poMx1 expression

Virus NP synthesis from infections of Vero cells that had been transiently transfected by plasmids encoding either eGFP (negative control), huMxA (positive control), or poMx1 was assayed, and the results are shown in Figure 2 (A–B). Given the reproducibility of the infection rate among nonexpressing cells between experiments (white boxes in Fig. 2B), whatever the plasmid tentatively incorporated was, we assume that the transfection procedure itself equally affected the cell populations transfected/infected. Moreover, as the infection rate of eGFP-expressing cells tended to be higher than that of nonexpressing

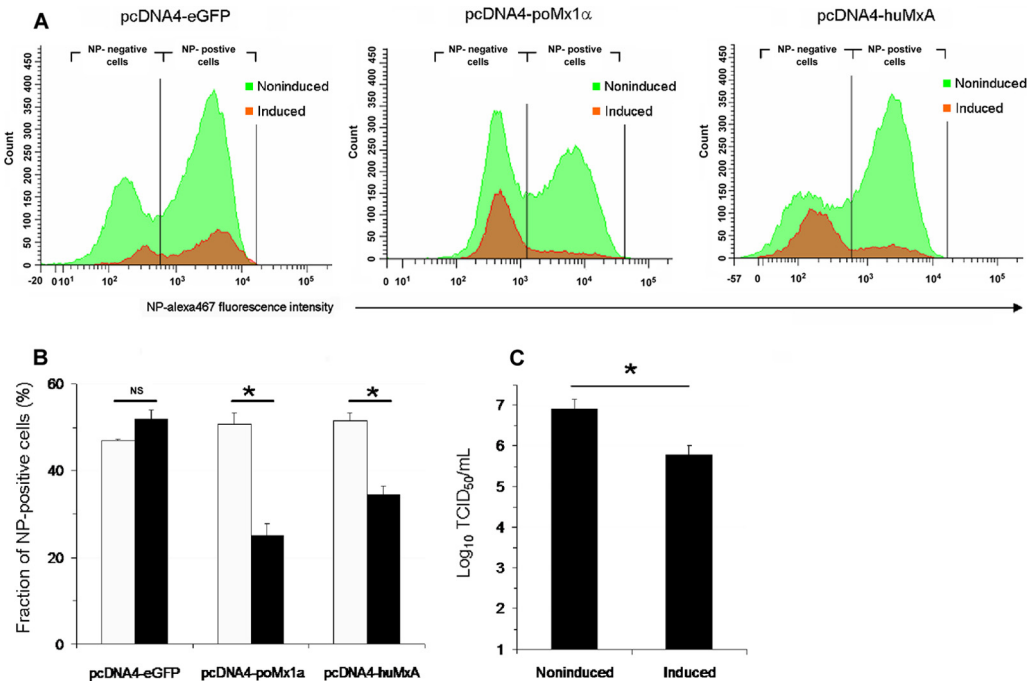

Figure 2. Porcine Mx1 expression alters influenzavirus NP synthesis (A–B) and production of infectious progeny particles (C). A–B: flow cytometric determination of NP-positive counts in Vero cells transfected with plasmids (pcDNA4) encoding either eGFP (negative control), porcine Mx1 (poMx1α) or human MxA (huMxA, positive control). (A) Example. Cell counts (vertical axis) refer to infected (NP-positive) and noninfected (NP-negative) cells detected in induced (transgene-expressing, dark grey) and non-induced (nonexpressing, light grey) cell populations. (B) Percent NP-positive cells 5 hpi in transgene-expressing (black boxes) and nonexpressing (white) cells. The corresponding plasmids had been transfected 24 h before infection, each population process resulting in a mixed population of expressing and nonexpressing cells. Cells were permeabilized, double immunostained for Mx proteins and virus NP and analysed using the FACS Canto, gating on the forward and side scatter to exclude debris and collecting fluorescences in FL-1 and FL-5. A minimum of 10 000 events were acquired and analyzed with BDFACSDiva software v4.1.1. Each box pair (white/black) represents means ± SD in nonexpressing/expressing cells from 3 independent experiments. Expression of both porcine and human MxA resulted in a significant decrease of NP-positive cell counts at the timepoint studied (5 hpi). (C) Influenza virus yields from stably-transduced porcine Mx1-expressing Vero cell monolayers were significantly decreased after induction of poMx1 expression. Pools of induced (black boxes) and non-induced (white boxes) V50 cells were infected with the H1N1 virus for 48 h (m.o.i. = 0.01). The viral titers in the culture supernatants are plotted, as determined in triplicate by standard median tissue culture infectious dose assays. TCID50: 50% tissue culture infective dose. Plotted values are means ± SD of 3 independent experiments. *Significantly different from the titer retrieved from the corresponding non-induced cells, $p < 0.05$. (A color version of this figure is available on line at www.vetres.org.)

cells, it is deduced that the transduction process per se did not alter the virus biological cycle in the cell preparations studied (Fig. 2B). The systematic depletion ($p < 0.01$) of NP-positive cells among MX-expressing cell populations (black boxes in Fig. 2B) is therefore attributable to the Mx proteins themselves.

Furthermore, viral yields from infections of non-induced and induced stably transduced V50 cells were assayed, and the results are

shown in Figure 2C. Porcine Mx1 expression caused a significant (~ 10 times) reduction in virus infectious particle yields. No titer reduction was observed when Vero/TetR1 cells were infected, with or without addition of doxycycline (data not shown), suggesting that the resistance conferred is attributable to poMx1 expression.

3.3. Upon poMx1 expression, viral protein production is blocked before early translation

For the first 9 h after infection, synthesis of the viral NP was monitored by immunofluorescence in V50 cells induced or not with doxycycline (Fig. 3). Non-induced cells followed a very reproducible scenario: at 4 h post-infection (pi), a weak but undeniable NP-specific signal was perceptible in a very small minority of the nuclei; at 5 hpi, between a third and a half of the nuclei showed intense, homogeneous staining, with only the nucleoles remaining NP-negative. At 6 hpi, 90% of the nuclei were NP-positive and NP had begun to spread to the cytoplasm. In all cells showing a cytoplasmic signal, the nuclei showed a "centrifugal" staining pattern, with an NP-negative center and a conspicuously NP-positive nucleoplasmic margin. After 7 hpi, most cells showed intense cytoplasmic labeling, and some nuclei had become NP-negative. Doxycycline-induced V50 cells, on the other hand, showed delayed and much lower NP synthesis as compared to non-induced cells (Fig. 3). We conclude that the mechanism (or one of the mechanisms) by which poMx1 inhibits influenza A viruses enters in action before or during translation of NP transcripts.

3.4. Upon poMx1 expression, viral mRNA production is blocked before primary transcription

To see if poMx1 affects translation of viral mRNA, we measured the level of NP transcripts available for translation. For this we performed reverse-transcription real-time PCR on extracts of infected V50 sampled 3 hpi. After optimization, the amplification efficiency remained constant over a range spanning 5 orders of magnitude for both 18S (R^2 = 0.9207) and NP (R^2 = 0.947) RNA transcripts. As compared to their poMx1-nonexpressing counterparts, poMx1-expressing cells showed an approximate 65% decrease in the level of NP-encoding transcripts available for translation (Fig. 4). As the final NP transcript level is the result of both primary transcription (of the initial parental genomes) and secondary transcription (of progeny vRNP), we repeated the experiment in the presence of cycloheximide to see if the block occurs before or after primary transcription. In the presence of cycloheximide, poMx1 expression still caused a strong decrease (~ 40%) in the NP transcript level (Fig. 4). We conclude that poMx1 inhibits the influenza A virus cycle before primary transcription.

3.5. Generation of virion-containing late endosomes is inhibited/delayed upon poMx1 expression

To see if poMx1 exerts its inhibitory effect on parental vRNP injection into the cytoplasm from the late endosomes or on the translocation of these vRNP from the cytoplasm to the nucleus, we examined whether poMx1 can alter the post-infection perinuclear accumulation of late endosomes. For this we specifically labeled the cell membranes by incubating the cells in DiD, a lipophilic dye. Each time non-induced V50 cells were processed in this manner and then infected for 40 min, the same pattern of intense perinuclear staining was observed, suggesting the occurrence of massive endocytosis followed by centripetal trafficking and perinuclear accumulation of membranes and endocytosed virions (Fig. 5). In contrast, induced V50 cells showed much weaker to no perinuclear staining. This suggests that poMx1 blocks or delays an event preceding perinuclear accumulation of particles internalized into late endosomes (Fig. 5).

After internalization, influenza A virions are transferred first to early endosomes, then to late endosomes, where acidification leads to an irreversible conformational change in the viral

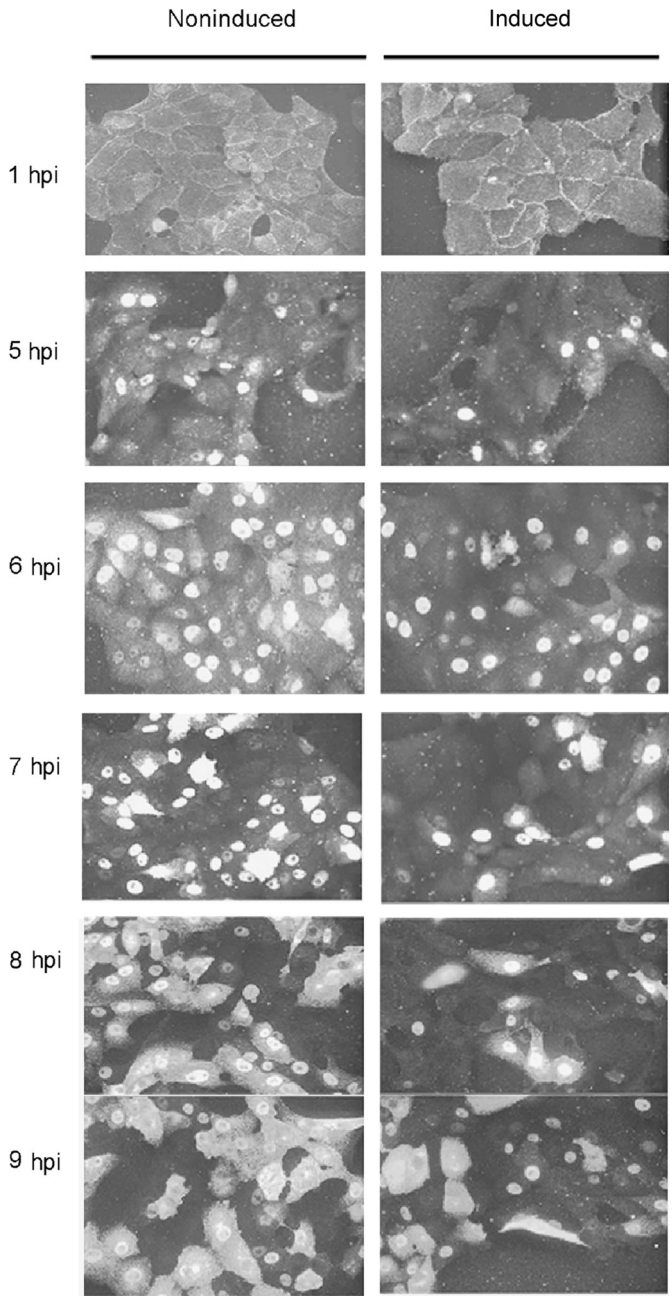

Figure 3. De novo synthesis of H1N1 influenza A virus nucleoprotein (NP) is delayed by porcine Mx1 expression. Production of viral NP by induced and non-induced V50 cells was monitored for 9 h after infection by indirect immunofluorescence, after sequential incubation with the anti-NP mAb from Abcam and Alexa 488-conjugated goat anti-mouse IgG. See text for detailed comparative analysis of NP production scenario in induced and non-induced cells.

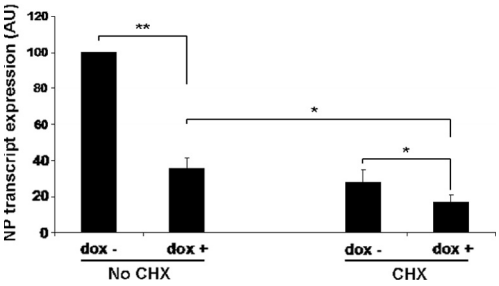

Figure 4. Porcine Mx1 blocks the influenza A virus life cycle before primary transcription. Cell monolayers were infected with the H1N1 influenza A virus strain for 3 h. Production of transcripts encoding H1N1 influenza A virus NP was quantitated by reverse transcription and real-time PCR in induced and non-induced V50 cells exposed or not, as indicated, to the translation inhibitor cycloheximide (CHX, 100 μg/mL). 18S rRNA was used as an internal control to normalize NP transcript data, and results were expressed percentages of the amount of NP transcripts retrieved from non-induced and nonexposed V50 cells, i.e. the only cells in which the virus life cycle proceeds unhindered. In the absence of CHX, poMx1 expression caused an approximately 65% reduction of NP-encoding mRNA production, and an approximately 40% reduction was still observable after exposure to CHX. Plotted values are means ± SD of triplicate real-time PCR assays, and three independent experiments were performed, with similar results. Fisher's exact test was used to compare the means and the reported significance levels are $p < 0.05$ (*) and $p < 0.01$ (**). AU: arbitrary units. See text for detailed interpretation.

hemagglutinin (HA). Accordingly, inhibited or delayed transport from primary endocytic vesicles into late endosomes should result in diminished or delayed adoption of the "acidic" conformation of influenza A virus HA. When non-induced V50 cells were immunostained 40 min pi with the conformation-specific mAb A2 specifically targeting acidic HA, a bright perinuclear signal was observed, as expected (Fig. 6). Similarly immunostained induced V50 cells showed only a faint, if any, signal. Taken together, these two experiments show that accumulation of incoming virions in perinuclear late endosomes is inhibited or delayed by poMx1.

3.6. Generation of virion-containing primary endocytic vesicles is not affected by poMx1

To see whether poMx1 hinders binding and internalization of incoming virions, the above experiment was repeated except that infection was stopped only 10 min pi and that the cells were immunostained with the conformation-specific mAb N2, which specifically targets the "neutral" conformation of HA. In this case the HA immunofluorescence signature was identical whether the cells were exposed to doxycycline or not, with preferential labeling of the cell periphery (Fig. 6).

3.7. The size, number, and spatial distribution of EEA1-positive subcellular structures are altered upon poMx1 expression

Early endosome autoantigen 1 binds to phosphatidylinositol-3,4,5-triphosphate (PIP3) and localizes, together with Rab5, to primary endocytic vesicles and early endosomes at the cell periphery. It is thus a good marker of the integrity of the early segment of the endocytic pathway. Immunostaining of EEA1 in non-induced V50 cells reproducibly revealed a finite number of distinct, bright spots, whereas staining was always weak and diffusely distributed in doxycycline-induced cells (Fig. 7).

4. DISCUSSION

Pig cells express two different Mx proteins, poMx1 and poMx2, upon IFN-α treatment [20]. We have demonstrated that poMx1 decreases or delays NP synthesis, and inhibits production of progeny viral particles. Among the various blocks theoretically possible, we have shown that poMx1 already hampers viral infection at an early stage and we attempted to identify the limiting early step. Specific transport processes provide excellent targets for interference with influenza virus life cycle [31]. Here we present evidence that poMx1 blocks the normal centripetal movement of incoming viral particles into the nucleus by interfering with an early step of the endocytic pathway: it would appear to alter either the

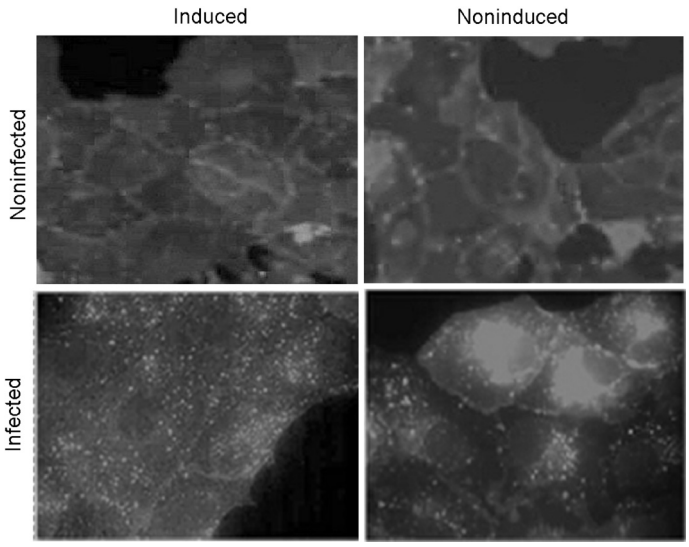

Figure 5. Porcine Mx1 expression inhibits the centripetal traffic of endocytic vesicles containing incoming influenza A virus particles. Twenty minutes after addition of the lipophilic dye DiD to the medium, an inoculum drawn from the H1N1 influenza A virus stock and corresponding to a multiplicity of infection of $\sim$ 200 was added to induced and non-induced V50 cells. Infection was stopped 40 min after infection by thorough PBS washings and fixation of cell monolayers with 4% paraformaldehyde. No additional staining was done, so the only visible fluorescence signals are from endocytosed fragments of plasma membrane and viral particles. Forty minutes after infection, non-induced cells displayed endocytosed material concentrated around the cell nuclei. Induced cells, in contrast, reproducibly displayed a diffuse, punctate, ''dusty'' pattern compatible with a block in the normal centripetal traffic of endocytosed materials.

normal recruitment of EEA1 to early endosomes or the number, morphology, and spatial distribution of early endosomes. We base this conclusion on the results of several successive experiments.

Firstly, as poMx1 is cytoplasmic and as the synthesis of both NP protein and NP transcripts is strongly inhibited in the presence of poMx1, the viral cycle must be hindered either before transcription or between primary and secondary transcription. Use of the translation-inhibiting agent cycloheximide has enabled us to show that a blockade occurs upstream from transcription. When influenza-A-virus-infected cells are exposed to cycloheximide, the absence of de novo synthesis of the viral proteins NP, PB1, PB2, and PA prevents polymerization of the negative progeny-genome RNA strands from cRNA strands [4, 41, 43]. Hence, by comparing the NP transcript levels observed in the presence and absence of cycloheximide, it is possible to distinguish a pretranscriptional block (which should affect the levels of transcripts resulting from transcription of both parental and neosynthesized matrices) from an intratranscriptional block (which should affect only those resulting from transcription of neosynthesized matrices). Our results reveal unambiguously that in the presence of poMx1, the viral cycle is already inhibited before primary transcription, thus before injection of vRNP into the nucleus. As the only available study to have addressed the anti-influenza mechanism of a cytoplasmic Mx protein, human MxA, led to the conclusion that the virus cycle is blocked after primary transcription [27, 44], the present results highlight the functional diversity among mammalian Mx proteins.

Before becoming available for primary transcription in the nucleus, parental vRNP undergo

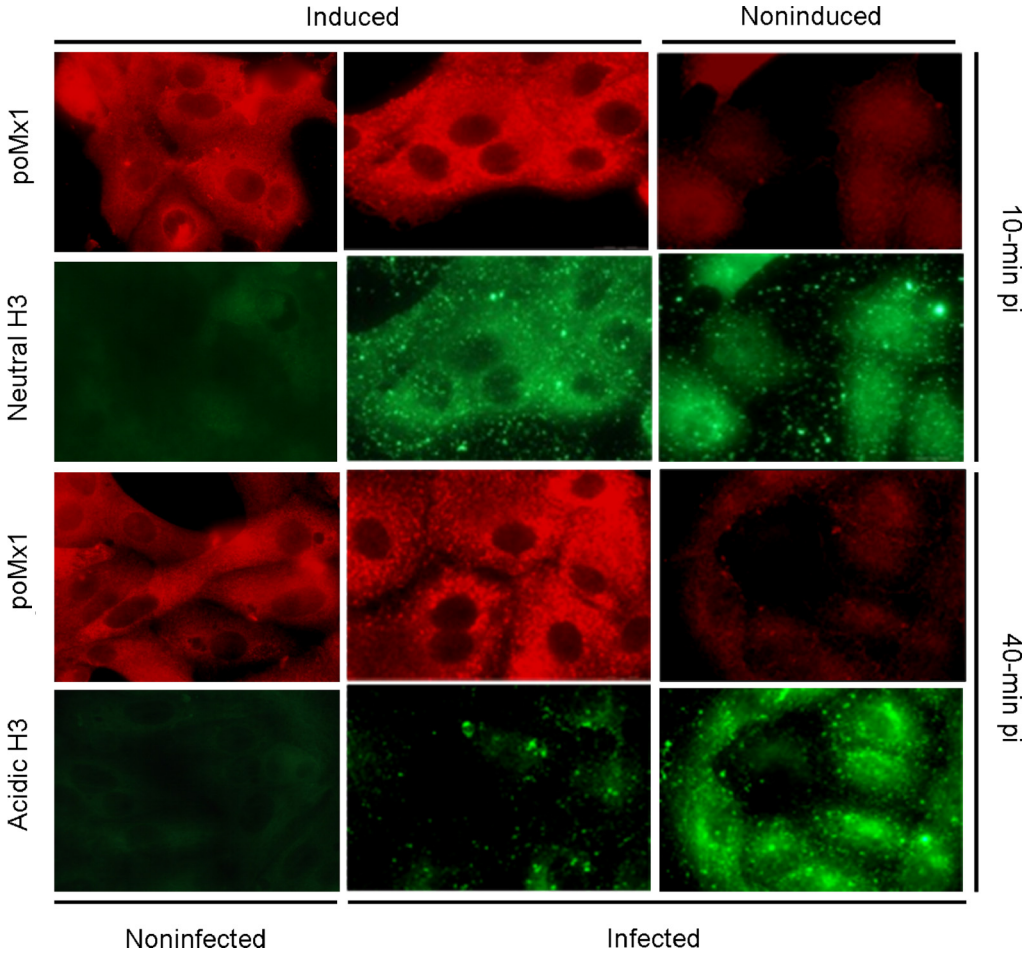

Figure 6. The traffic of incoming viral particles is blocked by poMx1 after internalization but before the acidification-induced conformational change of viral hemagglutinin in the late endosomes. Induced and non-induced cell monolayers were infected with a dilution of the H3N2 influenza A virus stock (m.o.i. ~ 200) and examined 10 min (upper half) and 40 min (lower half) pi after immunostaining of poMx1 (in red) or viral HA (in green). Ten minutes pi, internalized viral particles were detected by labeling the neutral form of the viral HA with N2 mAb. The results are similar for induced and non-induced cells. Forty minutes pi, internalized virus particles having arrived in the perinuclear region were detected by labeling the acidic HA form, this time with the A2 mAb. Non-induced cells show conspicuous staining of acidic HA in the perinuclear region, but induced cells do not. In the latter, traffic to the late endosomes is thus delayed. (A color version of this figure is available on line at www.vetres.org.)

a multi-step transport process involving: (i) binding and (ii) receptor-mediated endocytosis of the viral particle, (iii) docking and fusion of primary endocytic vesicles and early endosomes, (iv) early endosome fragmentation and generation of endosomal carrier vesicles, (v) movement towards and fusion with late endosomes, (vi) acidification-dependent fusion of viral and late endosomal membranes and subsequent delivery of the virus genome to

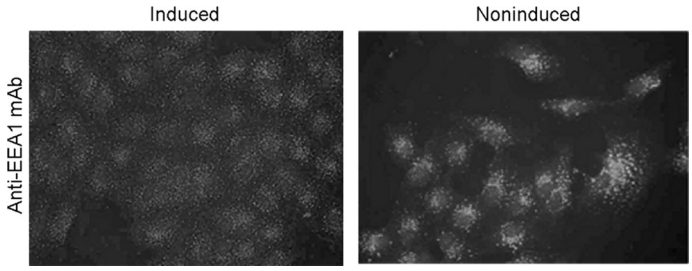

Figure 7. Porcine Mx1 expression alters the spatial distribution of structures bearing the early endosome autoantigen 1 (EEA1). Early endosomes were immunostained by sequential incubation with a mAb targeting EEA1 and with an Alexa 488-conjugated goat anti-mouse IgG. Numerous distinct bright granules are visible in non-induced cells, corresponding to early endosomes. Only a diffuse, "dusty" pattern is seen when poMx1 is expressed.

the cytoplasm, and (vii) translocation of vRNP into the nucleus [1, 10, 11, 14, 17, 18]. To identify the limiting step of this centripetal traffic in the presence of poMx1, we have used two independent approaches, both aiming to establish whether the virus cycle takes place as usual from the time the infecting viruses bind to the cell until the viral particles reach the late endosomes. The design of these experiments is inspired from the results of other teams, showing that by 40 min pi, the great majority of incoming viral particles have colocalized with late endosomal markers in close proximity to the cell nucleus [33]. In our first experiment, both induced and non-induced V50 cells were exposed to a lipophilic fluorescent dye, DiD, shortly before infection. Under these conditions, perinuclear fluorescent label was detected 40 min pi in the absence of poMx1, but not in the poMx1-expressing cells. As plasma membranes are intrinsically impermeable to DiD, the fluorescent spots observed in the cytoplasm must necessarily reflect the presence of membrane fragments internalized by endocytosis during concomitant exposure of the cells to both DiD and the virus. Hence, the diffuse DiD retention observed at the cell periphery in the presence of poMx1 suggests blocking of the centripetal traffic of primary endocytic vesicles to the perinuclar late endosomes. The second battery of experiments imagined to examine the centripetal traffic of incoming viral particles consisted in examining whether the shift of viral hemagglutinin to its acidic conformation is influenced by the presence of poMx1. To carry out this experiment, we took advantage of the mAb A2 known to target specifically the acidic conformation (adopted below pH 6.0) of hemagglutinin H3 of strain X-31 [33, 38]. Once again, striking differences appeared between non-induced and poMx1-expressing V50 cells: in the former, many bright agglutinated spots were seen in close proximity to the nucleus, whereas the latter cells showed no significant labeling. Since in the course of their normal cycle virions are exposed to a gradually decreasing pH, occurring when they are transferred from the early to the late endosomes and responsible for the conformational change of hemagglutinin, we conclude that in the presence of poMx1, the hemagglutinins of the incoming virions have not yet adopted their acidic conformation at a time when those of non-induced cells already have. Taken together, these two experiments demonstrate that the centripetal traffic of primary endocytic vesicles and their content is slowed down in the presence of poMx1. In particular, perinuclear agglutination of incoming virions does not occur within the standard time span (40 min). We then examined whether induced and non-induced cells might differ as regards binding and/or internalization of infecting virions. This time we used mAb N2, known to recognize specifically the "neutral" conformation (adopted above pH 6.0) of viral hemagglutinin [33, 38].

In several independent experiments, and whether the V50 cells were induced or not, infecting virions were observed at the cell periphery 10 min pi, as observed by others [33]. The poMx1 protein thus does not affect binding and internalization of incoming virions, as observed previously for human MxA [32].

Now that it appears established that poMx1 blocks the viral life cycle after internalization but before acidification in the late endosomes, we can suspect hindering of (i) docking and fusion of virus-containing primary endocytic vesicles and early endosomes, (ii) the traffic of the endosome transport carrier vesicles that fragment off from the early endosome and translocate towards the cell center, or (iii) coalescence of endosome transport carrier vesicles with late endosomes [5, 23, 28, 42]. As early endosomes constitute the first sorting station on which many routes of endocytosis converge [19] and because influenza-A-virus-containing primary endocytic vesicles translocate to them [33], we then gave priority to examining this step. Docking of primary endocytic vesicles to early endosomes and their fusion with them are regulated mainly by the GTP-bound Rab5 on the donor membrane and PIP3 on the acceptor membrane. These molecules then function as a "coincidence" signal for recruitment of the cytoplasmic protein EEA1, which cross-links the two membranes [6, 25, 35, 39]. We therefore examined the topological distribution of EEA1-positive subcellular structures upon poMx1 expression. As described in the literature [30], we identified many EEA1-positive spots at the periphery of non-induced V50 cells. In the presence of poMx1, this typical pattern was abolished. One possible interpretation is that poMx1 interferes with the action of EEA1, which is indispensable to docking, to fusion of virion-containing primary endocytic vesicles to early endosomes, and to their motility along microtubules [28]. This would block at least partially a key step in the centripetal traffic of incoming viral particles. How, exactly, poMx1 could prevent normal association of EEA1 with primary endocytic vesicles and early endosomes at the molecular level remains to be determined. Imaginably, mono- or multimeric poMx1 might wrap around one or both of EEA1′s "receptors", GTP-bound Rab5 and PIP3, preventing local accumulation of EEA1 and dramatically inhibiting its ability to tether primary endocytic vesicles to early endosomes. Alternatively, poMx1 might cause depletion of either Rab5-GTP or PIP3. If so, and if the affinity of EEA1 for either of these components is low or if at least one of them is labile, EEA1 binding to membranes could be inefficient. Another interpretation compatible with the observed fluorescence pattern is that the early endosomes undergo spatial redistribution and a reduction in size. It is noteworthy in this regard that exposure of MDCK cells to nocodazole, a microtubule-depolymerizing agent, generates exactly the same changes in the EEA1 staining pattern as observed here in poMx1-expressing Vero cells [7]. The poMx1 protein might thus exert a nocodazole-like effect, for instance by disorganizing the microtubule networks, which would delay the centripetal migration/maturation of carrier endosomes containing incoming viral particles. The credibility of this hypothesis is reinforced by the recent demonstration by immunoprecipitation of the existence of close molecular interactions between the human MxA protein and tubulin [21]. It is noteworthy that 1 h after infection of poMx1-expressing cells, a specific immunostaining pattern was observed, consisting of bright spots lining the plasma membrane, accentuating the "tiled" aspect of the cell preparations (Fig. 3). Interestingly, this pattern is compatible with "stagnation" of recently internalized virus-containing endocytic vesicles at the cell periphery. It resembles surprisingly the typical images obtained after high-dose influenza virus infection when endocytosis is blocked with wortmannin [8, 13], a PI3K inhibitor blocking PIP3 synthesis and thereby abolishing EEA1 binding. In any case, the present results reveal a type-I-IFN-triggered antiviral activity that aborts viral infection at an early stage of infection. Because it prevents early viral gene expression and genome replication, preventing proper intracellular transport may

be a host defense strategy more resistant than others to the rapid emergence of resistant virus variants.

Acknowledgements. We thank Michaël Sarlet and Grégory Pire for enthousiast logistical and skilled technical support. This work was supported by the Interuniversity Attraction Poles, phase VI, project P6/14 (GPCRs) and by the EU-funded Network of Excellence EADGENE. M. Palm is a Research Fellow of the "Fonds pour la Recherche dans l'Industrie et l'Agriculture", Brussels, Belgium.

REFERENCES

[1] Apodaca G., Endocytic traffic in polarized epithelial cells: role of actin and microtubule cytoskeleton, Traffic (2001) 2:149–159.

[2] Arnheiter H., Haller O., Antiviral state against influenza virus neutralized by microinjection of antibodies to interferon-induced Mx proteins, EMBO J. (1988) 7:1315–1320.

[3] Baise E., Pire G., Leroy M., Gérardin J., Goris N., De Clercq K., et al., Conditional expression of type I interferon-induced bovine Mx1 GTPase in a stable transgenic vero cell line interferes with replication of vesicular stomatitis virus, J. Interferon Cytokine Res. (2004) 24:513–521.

[4] Barret T., Wolstenholme A.J., Maby B.W.J., Transcription and replication of influenza virus RNA, Virology (1979) 98:211–225.

[5] Bucci C., Parton R.G., Mather I.H., Stunnenberg H., Simons K., Hoflacks B., Zerial M., The small GTPase rab5 functions as a regulatory factor in the early endocytic pathway, Cell (1992) 70:715–728.

[6] Christoforidis S., McBride H.M., Burgoyne R.D., Zerial M., The Rab5 effector EEA1 is a core component of endosome docking, Nature (1999) 397:621–625.

[7] D'Arrigo A., Bucci C., Toh B.H., Stenmark H., Microtubules are involved in bafilomycin A1-induced tubulation and Rab5-dependent vacuolation of early endosomes, Eur. J. Cell Biol. (1997) 72:95–103.

[8] Ehrhardt C., Marjuki H., Wolff T., Nürnberg B., Planz O., Pleschka S., Ludwig G.S., Bivalent role of the phosphatidylinositol-3-kinase (PI3K) during influenza virus infection and host cell defence, Cell. Microbiol. (2006) 8:1336–1348.

[9] Emeny J.M., Morgan M.J., Regulation of the interferon system: evidence that Vero cells have genetic defect in interferon production, J. Gen. Virol. (1979) 43:247–252.

[10] Goldstein J.L., Brown M.S., Anderson R.G.W., Russel D.W., Schneider W.J., Receptor-mediated endocytosis: concepts emerging from LDL receptor system, Annu. Rev. Cell Biol. (1985) 1:1–39.

[11] Gruenberg J., The endocytic pathway: a mosaic of domains, Nat. Rev. Mol. Cell Biol. (2001) 2:721–730.

[12] Huang T., Pavlovic J., Staeheli P., Krystal M., Overexpression of the influenza virus polymerase can titrate out inhibition by the murine Mx1 protein, J. Virol. (1992) 66:4154–4160.

[13] Kjeken R., Mousavi S.A., Brech A., Griffiths G., Berg T., Wortmannin-sensitive trafficking steps in the endocytic pathway in rat liver endothelial cell, Biochem. J. (2001) 357:497–503.

[14] Klasse P.J., Bron R., Marsh M., Mechanisms of enveloped virus entry into animal cells, Adv. Drug Deliv. Rev. (1998) 34:65–91.

[15] Lindenmann J., Resistance of mice to mouse-adapted influenza A virus, Virology (1962) 16:203–204.

[16] Lindenmann J., Inheritance of resistance to influenza virus in mice, Proc. Soc. Exp. Biol. Med. (1964) 116:506–509.

[17] Martin K., Helenius A., Transport of incoming influenza virus nucleocapsids into the nucleus, J. Virol. (1990) 65:232–244.

[18] Matlin K.S., Reggio H., Helenius A., Simons K., Infectious entry pathway of influenza virus in canine kidney cell line, J. Cell Biol. (1998) 91:601–613.

[19] Maxfield F.R., McGraw T.E., Endocytic recycling, Nat. Rev. Mol. Cell Biol. (2004) 5:121–132.

[20] Müller M., Winnacker E.L., Brem G., Molecular cloning of porcine Mx cDNAs: new members of a family of interferon-inducible proteins with homology to GTP-binding proteins, J. Interferon Res. (1992) 12:119–129.

[21] Mushinski J.F., Nguyen P., Stevens L.M., Khanna C., Lee S., Chung E.J., et al., Inhibition of tumor cell motility by the interferon-inducible GTPase MxA, J. Biol. Chem. (2009) 284:15206–15214.

[22] Nakajima E., Morozumi T., Tsukamoto K., Watanabe T., Plastow G., Mitsuhashi T., A naturally occurring variant of porcine Mx1 associated with increased susceptibility to influenza virus in vitro, Biochem. Genet. (2007) 45:11–24.

[23] Nielsen E., Severin F., Backer J.M., Hyman A.A., Zerial M., Rab5 regulates motility of early

endosomes on microtubules, Nat. Cell Biol. (1999) 1:376–382.

[24] Palm M., Leroy M., Thomas A., Linden A., Desmecht D., Differential anti-influenza activity among allelic variants at the *Sus scrofa* Mx1 locus, J. Interferon Cytokine Res. (2007) 27:147–155.

[25] Patki V., Virbasisus J., Lane W.S., Toh B.H., Shpetner H.S., Corvera S., Identification of an early endosomal protein regulated by phosphatidylinositol 3-kinase, Proc. Natl. Acad. Sci. USA (1997) 94:7326–7330.

[26] Pavlovic J., Zürcher T., Haller O., Staeheli P., Resistance to influenza virus and vesicular stomatitis virus conferred by expression of human MxA protein, J. Virol. (1990) 64:3370–3375.

[27] Pavlovic J., Haller O., Staeheli P., Human and mouse Mx proteins inhibit different steps of the influenza virus multiplication cycle, J. Virol. (1992) 66:2564–2569.

[28] Pfeffer S.R., Membrane traffic. Motivating endosome motility, Nat. Cell Biol. (1999) 1:E145–E147.

[29] Reeves R.H., O'Hara B.F., Pavan W.J., Gearhart J.D., Haller O., Genetic mapping of the Mx influenza virus resistance gene within the region of mouse chromosome 16 that is homologous to human chromosome 21, J. Virol. (1988) 62:4372–4375.

[30] Rubino M., Miaczynska M., Lippe R., Zerial M., Selective membrane recruitment of EEA1 suggests a role in directional transport of clathrin-coated vesicles to early endosomes, J. Biol. Chem. (2000) 275:3745–3748.

[31] Rust M.J., Lakadamyali M., Zhang F., Zhuang X., Assembly of endocytic machinery around individual influenza viruses during viral entry, Nat. Struct. Mol. Biol. (2004) 11:567–573.

[32] Shashidhar S.J., Mittal R., Expression of the antiviral protein MXA in cells transiently perturbs endocytosis, Biochem. Biophys. Res. Commun. (2004) 323:541–545.

[33] Sieczkarski S.B., Whittaker G.R., Differential requirements of Rab5 and Rab7 for endocytosis of influenza and other enveloped viruses, Traffic (2003) 4:333–343.

[34] Sieczkarski S.B., Brown H.A., Whittaker G.R., Role of protein kinase C beta II in influenza virus entry via late endosomes, J. Virol. (2003) 77:460–469.

[35] Simonsen A., Lippe R., Christoforidis S., Gaullier J.M., Brech A., Callaghan J., et al., EEA1 links PI(3)K function to Rab5 regulation of endosome fusion, Nature (1998) 394:494–498.

[36] Staeheli P., Haller O., Boil W., Lindenmann J., Weissmann C., Mx protein: constitutive expression in 3T3 cells transformed with cloned Mx cDNA confers selective resistance to influenza virus, Cell (1986) 44:147–158.

[37] Staeheli P., Grob R., Meier E., Sutcliffe J.G., Haller O., Influenza virus-susceptible mice carry Mx genes with a large deletion or a nonsense mutation, Mol. Cell. Biol. (1988) 8:4518–4523.

[38] Stegmann T., White J.M., Helenius A., Intermediates in influenza induced membrane fusion, EMBO J. (1990) 9:4231–4241.

[39] Stenmark K., Aasland R., Toh B.H., D'Arrigo A., Endosomal localization of the autoantigen EEA1 is mediated by a zinc-binding FYVE finger, J. Biol. Chem. (1996) 271:24048–24054.

[40] Stranden A.M., Staeheli P., Pavlovic J., Function of the mouse Mx1 protein is inhibited by overexpression of the PB2 protein of influenza virus, Virology (1993) 197:642–651.

[41] Taylor J.M., Illmensee R., Litwin S., Herring B., Broni B., Krug R.M., Use of specific radioactive probes to study transcription and replication of the influenza virus genome, J. Virol. (1977) 21:530–540.

[42] Vonderheit A., Helenius A., Rab7 associates with early endosomes to mediate sorting and transport of Semliki forest virus to late endosomes, PLoS Biol. (2005) 3:e233.

[43] Vreede F., Jung T., Brownlee G., Model suggesting that replication of influenza virus is regulated by stabilization of replicative intermediates, J. Virol. (2004) 78:9568–9572.

[44] Zürcher T., Pavlovic J., Staeheli P., Mechanism of human MxA protein action: variants with changed antiviral properties, EMBO J. (1992) 11:1657–1661.